Multiscale correlative tomography provides critical materials characterization of biomedical implants

Bartłomiej Winiarski[1,2], Grzegorz Pyka[1], Ali Chirazi[3]

1. Thermo Fisher Scientific (FEI Czech Republic s.r.o.), Vlastimila Pecha 12, Brno 627 00, Czech Republic; 2. Henry Moseley X-ray Imaging Facility, School of Materials, University of Manchester, M13 9PL, UK; 3. Thermo Fisher Scientific, 3, Impasse Rudolf Diesel, Bât A, F-33708 Mérignac, Bordeaux, France

INTRODUCTION

Correlative multiscale tomography (CMT)[1] is a new workflow that combines advanced imaging and analytical techniques to provide critical feedback to engineers designing new products, materials, and manufacturing processes. By combining and registering results from optical microscopy; micro X-ray computed tomography (μCT)[2]; EBSD, EDS/WDS, imaging and serial sectioning tomography (SST) with plasma focused ion beam/scanning electron microscopy (PFIB/SEM)[3]; and scanning/transmission electron microscopy (S/TEM), the workflow covers length scales from millimeters to angstroms and can provide three-dimensional (3D) analysis of characteristics ranging from surface roughness and porosity to composition and residual stress state[4]. To illustrate the power of the workflow, we describe here the analysis of a cellular material produced by an additive manufacturing (AM) process[5] to be used in a medical implant.

Titanium alloy implants are widely used to replace damaged bone. A leading cause of failure for these implants is stress shielding, in which bone loss results from a mismatch between the mechanical properties of the implant and the bone. Recently there has been considerable interest in the use of cellular titanium in this application[6,7]. Cellular in this context refers to materials that comprise a regularly repeating unit cell structure in a three-dimensional lattice. Such materials offer the opportunity to engineer the mechanical properties of the material by modifying components of the structure, such as the size, shape and arrangement of the structural members that constitute each cell. In the case of bone implants, a closer match between the properties of the bone and the implant can reduce stress shielding and associated bone loss, while the open lattice-like structure also permits the infiltration of bone tissue to strengthen the implant. The higher strength to weight ratios promised by cellular materials have also attracted considerable interest from the automotive and aerospace industries.

AM processes, sometimes referred to as 3D printing, have added impetus to the development of cellular materials and complex components by facilitating the translation of computer generated designs into real structures. AM processes such as selective laser melting (SLM), in which powdered particulates are fused into solid structures by the heat of a laser, can create complex structures quickly and easily; but the finished products show considerable variability in critical parameters, including cell member diameter, surface roughness, internal porosity, detrimental residual stresses and more.

To refine these processes and reduce variability, researchers need an efficient way to measure and inspect their products, and compare real-world results to design models. Importantly, they need multimodal, multiscale capability that incorporates multiple analytical techniques—imaging, composition, crystallography, residual stress testing and more; and extends over a range length scales—from millimeters to nanometers.

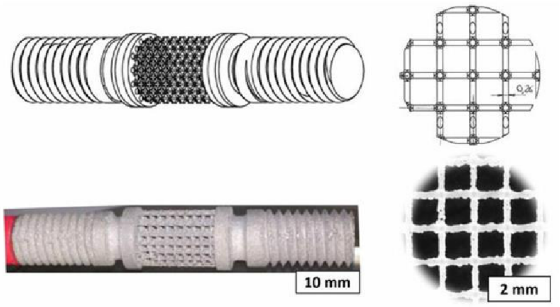

FIGURE 1 The CAD model and the implant cellular material actually produced by selective laser melting from Ti-6Al-4V ϕ~9 μm powder (top/bottom left). The details of cubic cellular scaffold is displayed on the right. Note the two screws are used in a fatigue study performed elsewhere[8]

CHALLENGES

AM processes are relatively new and not completely understood. They pose specific challenges, including a lack of standards, poor correspondence between the microstructural characteristics and mechanical performance of test coupons and produced components, a large number of process variables, and sensitivity to small changes in manufacturing parameters.

For example, Figure 1 shows the computer aided design (CAD) and finite element analysis (FEA) optimized model together with the actual implant material examined in this example. The cellular material is in the middle of the sample, while the screws at either end are there to facilitate macro mechanical testing, e.g. fatigue life inspection. At first glance, the AM produced structure appears to replicate the larger scale geometrical features of the CAD

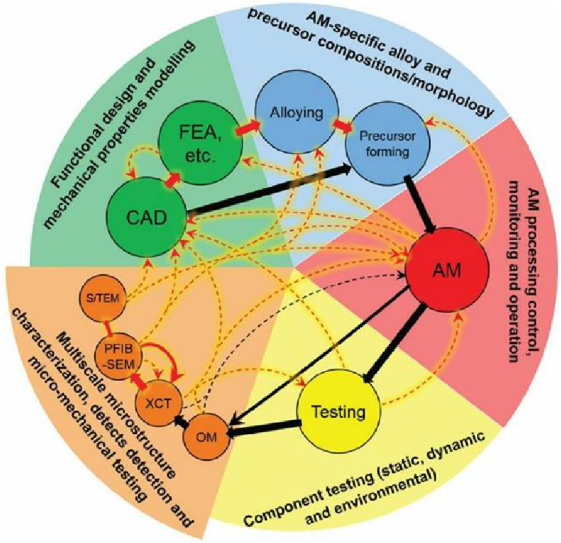

FIGURE 2 The product design, manufacture, test and inspection cycle (solid arrows) for additive manufacturing processes can be conveniently considered in five phases. All phases in this cycle of constant improvement benefit from feedback (dashed arrows) from various stages of microstructural analyses with multiscale correlative tomography. Solid black arrows indicate a typical cycle with dashed black arrows for the feedback, while an improved cycle is depicted with solid red arrows and the feedback marked with dashed red arrows

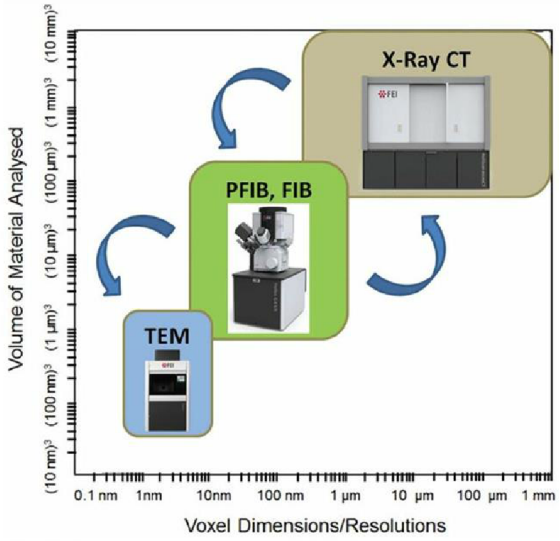

FIGURE 3 Typical 3D imaging methods for materials science used in Correlative Tomography Workflow. Arrows indicate sample transfer between instruments. Note: PFIB-SEM in the correlative workflow is a multipurpose platform for sample preparation (micro- nano CT pillars, blocks and slices for serial sectioning tomography, micro specimens for micro-mechanical testing, TEM lamellas), and for collection of various imaging modalities in 2D and 3D (SEM, EBSD, EDS, etc.)

design with a relatively high degree of fidelity. A closer look will reveal significant deviations. The ultimate goal of the design, manufacture, and test cycle we will describe is a complete understanding of the AM process, so the final product will closely match the designed performance, including geometry, composition, and mechanical behavior.

Design, manufacture, and test is a cycle of continuous improvement for which analytical feedback is critical at each step. It can be conveniently considered in 5 phases as shown in Figure 2, using solid red lines for the workflow steps and dashed red lines for the feedback loops. In the first iteration of the cycle CAD and FEA work together to optimize the design in terms of functionality and mechanical performance based on continuum elastic and isotropic modelling. This is followed by formulating the AM-specific alloy and processing it into a powdered precursor. Custom alloying is particularly important, since the powder fusion/melting process differs from thermodynamic states of material in classical metallurgy, and undesirable phases, inclusions, etc. may impair the designed microstructural features and mechanical performance. The laser fusion printing process follows, including monitoring and control of operational parameters, i.e. laser power, laser type laser beam shape, feed speed, melting paths, pre/post heating, remelting, powder ejecting, etc. It is important to record all processing parameter, since AM production takes dozens of minutes. Thus, any small variation of parameters reflected in the microstructural and mechanical characteristics will be easier to asses and control. Macro scale testing of static (tensile/compression), dynamic (fatigue, impact) and environmental performance (bio-compatibility) is next. Understanding significant deviations of microstructural and mechanical characteristics of AM test coupons from manufactured components currently poses a significant challenge at this phase of the cycle. The cycle closes with 3D microstructural characterization using CMT. This step can include micromechanical testing (e.g. micro-tensile testing, micro-pillar compression, micro residual stress measurements, etc.) that can be performed inside the PFIB-SEM instrument.

CORRELATIVE MULTISCALE TOMOGRAPHY WORKFLOW

As the name suggests, CMT correlates 3D information from tomographic analyses acquired over a range of scales (Figure 3). In practice, the workflow often includes multimodal data handling with precise co-localization of material volumes analyzed across different instruments, i.e. initial observations with optical microscopy at larger scales, envelope micro X-Ray CT inspection at macro/mezo-scale and PFIB SST analyses of sub-mm^3 volumes with nanometer resolution. If needed it can be extended to the atomic scale with TEM both 2D imaging and/or 3D nano-tomography. (TEM is not included in the examples presented here). The plasma (Xe+) FIB/SEM plays a unique and essential role in the workflow by bridging, macro, mezo, and nano scales in a way that has not been possible with liquid metal (Ga+) FIB-SEMs.

HELISCAN µCT

Computed tomography (CT) generally refers to a procedure in which images/projections of a sample positioned between a radiation source and a detector are acquired from different perspectives (or angular positions) and combined computationally to retrieve non-destructively details of structural features in a whole 3D volume. X-ray CT is widely familiar from its use in medical imaging, geology and wood study. Micro X-ray CT in life or materials sciences applies the same physical principles on a much smaller scale. The HeliScan µCT system used for this work implements a unique helical scan trajectory with a wide cone-beam angle and an iterative reconstruction algorithm to deliver high fidelity reconstructions with spatial resolution in the sub-micrometer range. These features allow scanning long specimens and reconstruct high contrast, low noise 3D volumes without stitching artifacts typically present in volumes reconstructed from circular scanning trajectories.

PLASMA XE+ DUALBEAM (PFIB/SEM)

The Helios DualBeam combines a Xe+ plasma focused ion beam (PFIB) column, used primarily for precise sample excision, with a monochromated scanning electron microscope (SEM) column, for high-resolution imaging. The system plays two essential roles in the workflow, first, as a high-resolution imaging and analysis tool, and second, as a sample preparation and manipulation tool that ties the workflow together. SEM imaging can resolve features down to the nanometer scale. Various detectors permit spatially resolved imaging and analysis of a range of sample characteristics, including surface topography contrast (typically secondary electrons detector), elemental composition (energy-dispersive X-ray spectroscopy - EDS), crystal orientation (electron backscattered diffraction patterns - EBSD) and atomic number contrast (typically backscattered electrons detectors).

The PFIB can also be used for ion imaging, but its most important contribution in this application is its ability to cut (mill) into, or deposit material on, the sample surface with nanometer scale placement precision

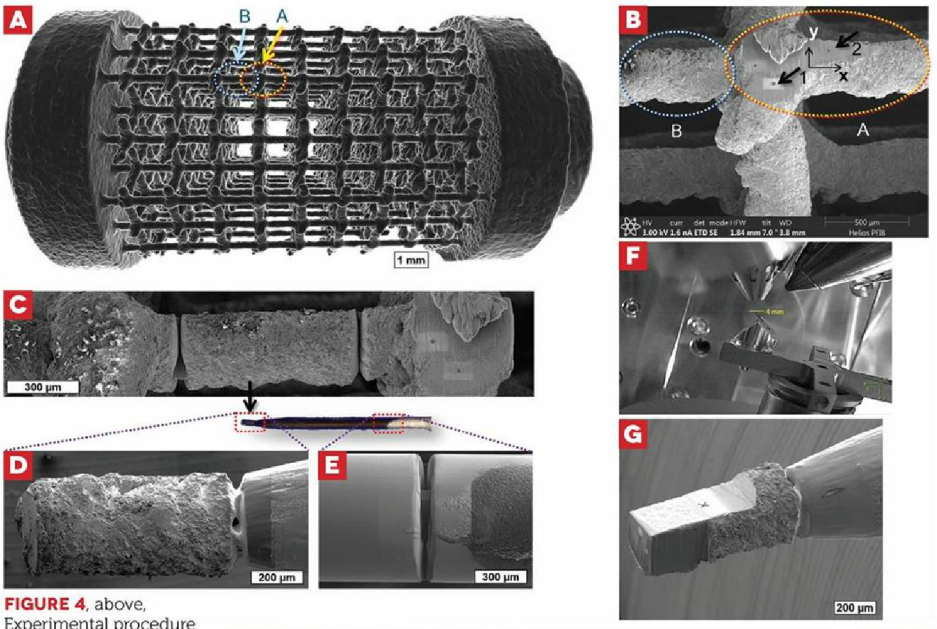

FIGURE 4, above, Experimental procedure of correlative multiscale tomography. (a) Visualization of the µCT envelope scan with a resolution of (4.8 µm)3/voxel; A – region for the micro residual stress mapping and B – region for high resolution µCT scan (b) close-up of the ROIs A and B from a), where arrows 1 and 2 show localization of the micro-holes; (c) resected strut from the scaffold before lift-out with the EasyLift; (d) the strut positioned on a pin for the high resolution µCT scan; (e) undercut pin with PFIB; (f) in-chamber view of a pin positioned on a pretilted stub used during PFIB-SEM SST; (g) the strut prepared for serial sectioning tomography data collection; note the two pores that were selected from µCT data

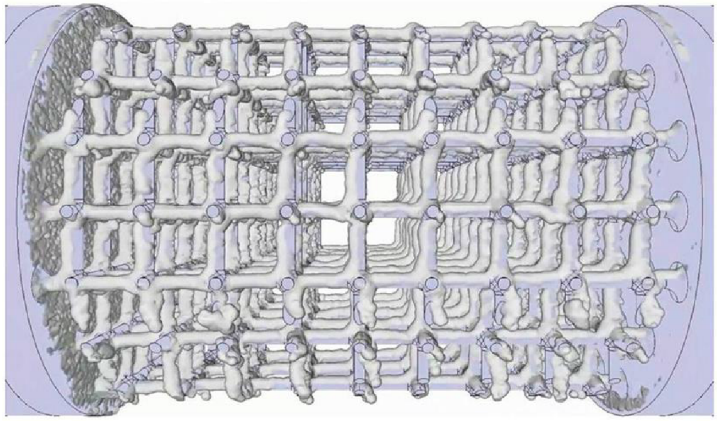

FIGURE 5, above right, the CAD model combined with the µCT envelop scan

and accuracy. The cutting action can be used to cross section the sample to reveal sub-surface features for imaging and analysis, prepare large micro-pillars for micro- and nano X-Ray CT imaging and excavate/prepare thin lamellas for TEM study. PFIB's high current (up to 2500 nA) Xe+ plasma focused beam increases the cutting speed to as much as 100 times more than Ga+ FIB. This is the key to its ability to span the size scales because it enables cross section sizes that are simply too large to be practical with Ga+ ion beams. Xe+ also has the advantage of being a noble gas, unlikely to interact chemically with sample atoms.

Serial section tomography (SST) uses a fully automated iterative cutting and imaging process, repetitively removing a thin layer of material from the sample with the PFIB and imaging/analyzing the newly exposed surface with the SEM, to create a stack of multimodal images from which the computer reconstructs a three-dimensional representation of the microstructure of specimen. PFIB SST analyzes a smaller volume than X-ray CT but can interrogate microstructural features, e.g. grains, grain orientations, grain boundaries and can achieve spatial resolutions down to the nanometer size range. Auto Slice & View software automates and simplifies the SST process.

The DualBeam system also includes an EasyLift nanomanipulator, which can be used to hold and position small and sub-millimeter pieces that have been cut free from the bulk sample. It is useful for positioning large blocks for slice-and-view tomography, for preparing lamellas for TEM analysis and for positioning of PFIB milled micro-pillars on micro CT sample holders.

EXPERIMENTAL PROCEDURE

The medical cellular scaffold analyzed here has a cubic elementary cell and has been CAD designed and FEA optimized to achieve an effective elasticity of 3 GPa, matching the elasticity of trabecular bone.

1) To characterize the implant sample, we begin at the larger scale with µCT envelop scan. The data acquisition took about 12h, while the 3D reconstruction algorithms needed another 5h to obtain a final voxel size of $(4.8\mu m)^3$.

2) After careful inspection we selected two regions of interest (ROI) containing internal pores for further study at higher resolutions (Figure 4a, b). Region A contains a strut that we will use for measuring axial and circumferential residual stresses using a PFIB-SEM based micro-hole drilling technique. To facilitate meaningful stress measurements, we removed material from area A to create a flat surface. Region B was selected for high-resolution µCT study. We resected the strut (~300µm diameter and 800 µm long) from the scaffold at B using PFIB and position it on a pin (Figure 4d) using the EasyLift™ nanomanipulator (Figure 4c, d, e).

3) We collected high-resolution µCT of the free-standing pin. The data acquisition took about 18h, and the 3D reconstruction required 3h to reach final voxel size of $(0.9\mu m)^3$.

4) We returned the strut-on-pin to the PFIB-SEM (Figure 4f) and use stage rotation to collect a series of secondary electron SEMs (~1 µm/pixel) from which we create a stereo photometric 3D SEM surface of the strut that we later use to co-localize multimodal data obtained from high-resolution µCT and PFIB-SEM SST volumes with positioning precision of < 3 µm.

5) Based on precise positioning from the µCT we prepared a site for PFIB-SEM SST (Figure 4f). Before the SST run we image the interior of the pores using through-lens detector in secondary electron mode (TLD-SE), then fill the pore with platinum using PFIB assisted deposition, to reduce curtaining artifacts that can develop edges and voids during FIB milling. The SST run included 4000 slices, each 25 nm thick (58 s. milling time). Every 4th cut the Auto Slice & View software collected a high-resolution SEM image for the subsequent reconstruction.

6) After the last slice we acquired a large area EBSD and high contrast SEM image using the annular backscattered electron detector.

RESULTS AND DISCUSSION

The envelop scan (Figure 5) provides valuable data itself and provides a basis for further analyses. Figure 6 shows the CAD model combined with the µCT envelop scan. Manufacturing defects, including missing parts of the scaffold are visible. Surface roughness and structural distortions in the produced structure are also apparent and depart significantly from the CAD model. In general, surface roughness is desirable

in medical scaffold, but excessive the surface roughness may promote structural instability.

Further investigation near regions A and B reveals number of internal defects (pores in Figure 6c and e) and mechanically weak areas, where the struts are much thinner than the CAD/FEA optimized cross-sections (260µm), in some areas as little as 100µm diameter (see cell wall diameter histogram in Figure 6d). However, the mode of strut thickness (310µm) is larger than designed (Figure 6d), which may lead to false mechanical predictions.

The scaffold contains many internal. roughly spherical pores (diameter 30-40 µm). Pores accounted for 0.8% of volume and are relatively uniformly distributed in the whole structure (Figure 6e). Region B containing two pores chosen for further correlative study is marked in Figure 6c and zoomed in image in Figure 6f shows one of the investigated pores (blue arrow) near the ligament junction.

Before resecting the strut from region B (Figure 4a), we measured the axial and circumferential residual stresses in region A (Figure 4b). We found detrimental tensile residual stresses of ~200 MPa along the strut and ~100 MPa on the circumference (Figure 6b). Tensile residual stresses can promote fatigue crack growth and reduce fatigue lifetime, leading to premature failure.

The envelop scan has the resolution of (4.8µm^3) per voxel, while the local scan of a strut-on-pin has the resolution of (0.9µm^3) per voxel. This gives richer and more accurate representation of the internal and external features of the strut, see Figures 7c and d. We used this high resolution µCT data (Figure 7f) together with stereo photometric 3D SEM surface (Figure 7e) to precisely position the ROI for PFIB-SEM serial sectioning tomography data collection. Figure 7g shows co-localized µCT data volume (blue) and the stereo photometric 3D SEM surface (gray).

High-resolution images of the pores revealed pore morphology largely deviates from spherical shape. The surface texture is complex and has areas that may act as stress concentrators (Figure 8c). During the cooling process of Ti-6Al-4V alloy high temperature Ti-β phase transforms to low temperature Ti-α' martensitic platelets microstructure. Since the trapped gas inside the material acts as a free-surface the martensitic platelets create stair-case like surface features, depicted in Figure 8d.

PFIB-SEM SST volume data is presented in Figure 8e. It has a voxel size of about (60nm)^3, providing much more information about external

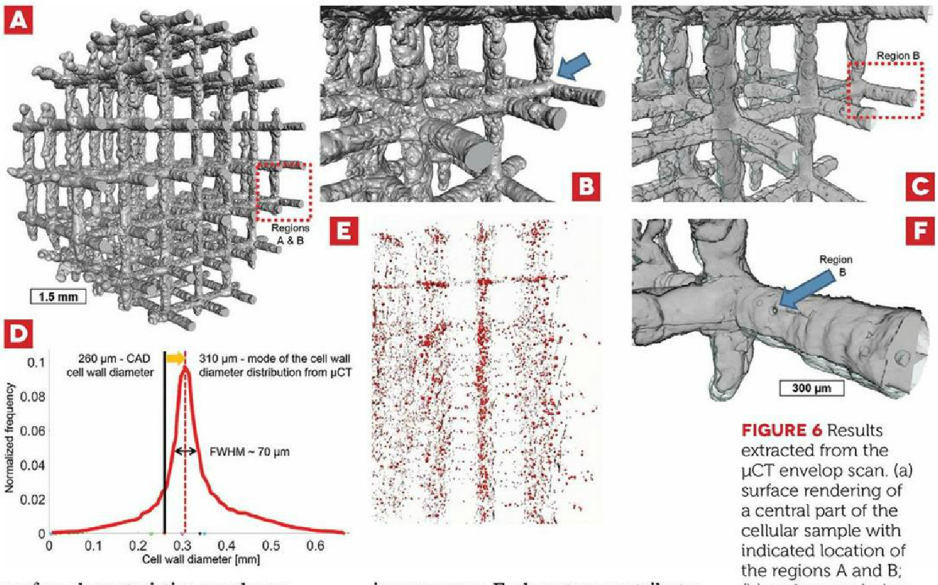

FIGURE 6 Results extracted from the µCT envelop scan. (a) surface rendering of a central part of the cellular sample with indicated location of the regions A and B; (b) surface rendering showing details of the printed surface, where blue arrow indicates thin area of a strut near a junction of the ROIs; (c) corresponds to b) and shows volume rendering with apparent internal pores; (d) cell wall diameter distribution; (e) surface rendering of the internal pores in the center part of cellular sample; (f) zoomed in region from c), where blue arrow indicates location the pores selected for further study

surface characteristics, roughness, micro voids, surface cracks and how these relate to the microstructure underneath. The data shows details of pore internal morphology (see Figure 8e). The 3D volume clearly shows Ti-α' martensitic platelets microstructure and traces of high temperature Ti-β phase, where Ti-α'platelets are oriented in a certain range of crystallographic orientations. This is depicted by 2D imagining using annular backscattered electron.

CONCLUSIONS

A correlative multiscale tomographic workflow combining helical µCT and PFIB-SEM can deliver multimodal analytical information across the length scales required to characterize and understand additive manufacturing processes. Each system contributes structural and analytical data directly, within its characteristic scale, and the PFIB-SEM also plays a key role in integrating the workflow across the full range of length scales. Although not addressed here, atomic scale S/TEM imaging and analysis is a logical extension of the workflow to still smaller scales. Our study correlates multiple/multiscale 3D imaging modalities to reveal the complexity of internal microstructure, defects/pores network and external surface characteristics of the AM medical scaffold. The scaffold characteristics vary significantly from the CAD model on number of levels. The workflow can provide critical feedback that will support designers' and engineers' efforts to refine the manufacturing process.

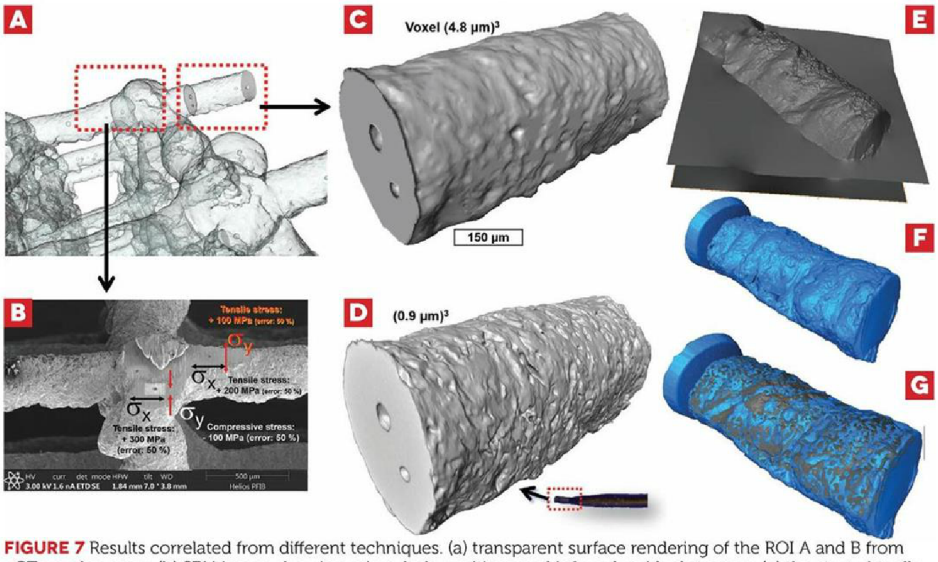

FIGURE 7 Results correlated from different techniques. (a) transparent surface rendering of the ROI A and B from µCT envelop scan; (b) SEM image showing micro-hole positions and inferred residual stresses; (c) the strut virtually resected from extracted µCT envelop scan data; (d) visualization of the strut µCT scanned on a pin; (e) the stereo photometric 3D SEM surface; (f) the strut µCT scanned on a pin before co-localization; (g) co-localized 3D data from e) and f)

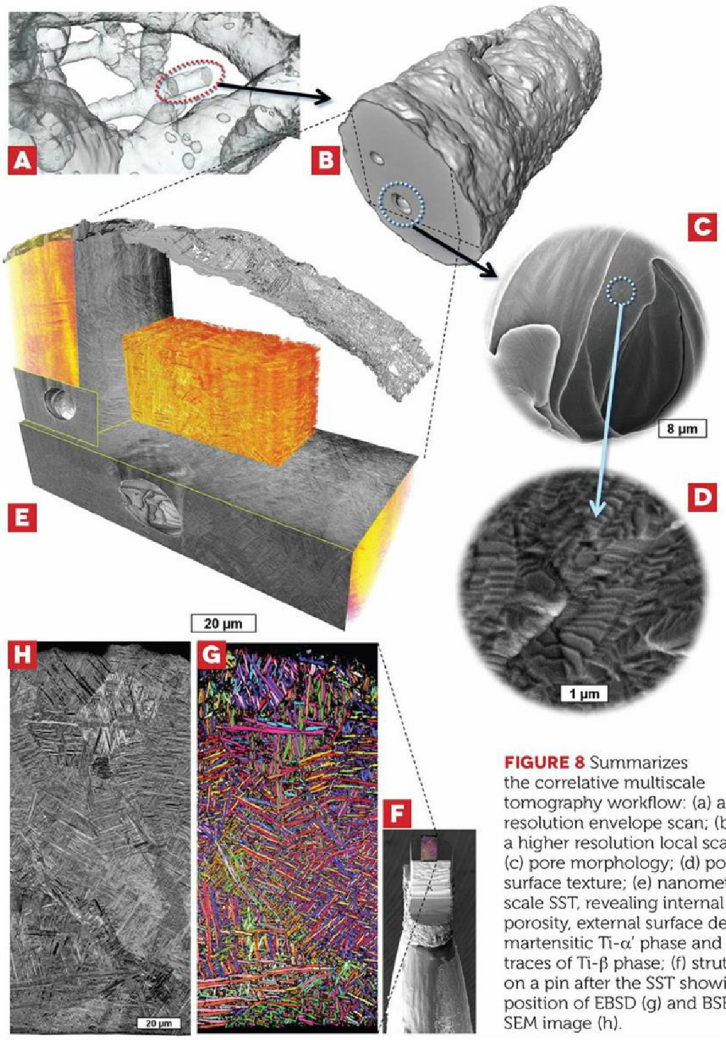

FIGURE 8 Summarizes the correlative multiscale tomography workflow: (a) a low-resolution envelope scan; (b) a higher resolution local scan; (c) pore morphology; (d) pore surface texture; (e) nanometer-scale SST, revealing internal porosity, external surface detail, martensitic Ti-α′ phase and traces of Ti-β phase; (f) strut on a pin after the SST showing position of EBSD (g) and BSE SEM image (h).

REFERENCES

1. Burnett, T.L., McDonald, S.A., Gholinia, A., Geurts, R., Janus, M., Slater, T., Haigh, S.J., Ornek, C., Almuaili, F., Engelberg, D.L., Thompson, G.E., Withers, P.J., Correlative Tomography. *Scientific Reports*, 2014. 4: p. 4711.
2. Withers, P. and E. Maire, Quantitative X-ray tomography. *International Materials Reviews*, 2014. 59(1): p. 1-43.
3. Winiarski, B., Burnett, TL, Kelley, R, Daly, M, Mani, K, Withers, PJ, Large volume high resolution Plasma FIB Serial Sectioning Tomography, in *The Microscience Microscopy Congress*, 29 June - 2 July 20152015: Manchester.
4. Benedetti, M., Fontanari, V, Winiarski, B, Allahkarami, M, Hanan , JC, Residual stresses reconstruction in shot peened specimens containing sharp and blunt notches by experimental measurements and finite element analysis. *International Journal of Fatigue*, 2016. 87: p. 102–111.
5. Benedetti, M., *et al.*, The effect of post-sintering treatments on the fatigue and biological behavior of Ti-6Al-4V ELI parts made by selective laser melting. *Journal of the Mechanical Behavior of Biomedical Materials*, 2017. 71: p. 295–306.
6. Wang, W. and C. Khoon Poh, Titanium Alloys in Orthopaedics, in Titanium Alloys - *Advances in Properties Control*, J. Sieniawski and W. Ziaja, Editors. 2013, InTech.
7. Tan, X., *et al.*, Metallic powder-bed based 3D printing of cellular scaffolds for orthopaedic implants: A state-of-the-art review on manufacturing, topological design, mechanical properties and biocompatibility. *Materials Science and Engineering C*, 2017. 76: p. 1328-1343.
8. Dallago, M., *et al.*, Fatigue properties of Ti6Al4V cellular specimens fabricated via SLM: CAD vs real geometry. *Structural Integrity Procedia*, In Review.

BIOGRAPHY

Dr. Bartlomiej (Bart) Winiarski is an applications scientist, (Materials & Structural Analysis) for Thermo Fisher Scientific, Brno, Czech Republic. He received his M.Sc. in Materials Science from AGH-University of Science and Technology, Krakow, Poland, and holds a Ph.D. in Mechanics of Composite Materials from the University of Aberdeen, Scotland. He received the R.E. Peterson Award from the Society of Experimental Mechanics (USA) in 2014 and has authored more than 30 peer-reviewed papers. From 2014 to 2016 he worked at the University of Manchester, School of Materials, as FEI Research Fellow where he explored the application of Plasma Xe+ FIB-SEM and Helical Micro X-Ray CT instruments to correlative multiscale/multimodal tomography in 3D materials science. He also developed novel methods for stress measurement at sub-micron scale using FIB-SEM and DIC techniques. Since 2016, he is a visiting academic at the University of Manchester, U.K.

ABSTRACT

Biological materials generally have complex three-dimensional (3D) hierarchical microstructures, which give rise to interesting combinations of anisotropic mechanical properties that often surpass those of manmade materials. Researchers seeking to develop man made analogs, to use as replacements for injured or diseased organs, or for use in a wide variety of extra-biological applications that leverage the materials' extraordinary properties, need to understand the structure of the materials they create over length scales ranging from millimeters to angstroms. We introduce a multi-modal, multi-scale analytical workflow that covers that range and combines spatial correlated results from an equally broad range of analytical techniques, including optical microscopy (OM), micro X-ray computed tomography (µCT), focused ion beam/scanning electron microscopy (FIB/SEM), electron backscattered diffraction (EBSD), energy/wavelength-dispersive X-ray spectroscopy (EDS/WDS), and more. The workflow-multiscale correlative tomography (MCT)-provides 2D/3D characterization that is critical to understanding of these structures and refining the processes we use to manufacture them. In this article, we describe the use of MCT to characterize as-manufactured imperfections, internal defects/pores and microstructural features of a Ti-6Al-4V titanium alloy medical cellular cubic scaffold manufactured with selective laser melting.

ACKNOWLEDGEMENTS

Authors acknowledge the EPSRC for grants EP/J021229/1 and EP/M010619/1 and BIS Capital Funding that established the Multiscale Characterization Facility – a part of Henry Moseley X-ray Imaging Facility. The authors gratefully acknowledge Regius Professor Philip J. Withers and Tim L. Burnett (University of Manchester, UK), Associate Professor Matteo Benedetti (University of Trento, Italy) and Dirk Laeveren (Thermo Fisher Scientific, NL) and Peter Westenberger (Thermo Fisher Scientific, France).

CORRESPONDING AUTHOR DETAILS

Bartlomiej.Winiarski@fei.com, Ali.Chirazi@fei.com and Grzegorz.Pyka@fei.com

Microscopy and Analysis 31(6): S4-S9 (AM), December 2017